Phase transformation kinetics of precursor gel to α-Alumina

T. NISHIO
Research & Development Center, and UNITIKA Research Laboratory, UNITIKA Ltd, 23, Uji-Kozakura, Uji-shi 611, Japan

Y. FUJIKI
National Institute for Research in Inorganic Materials, 1-1, Namiki, Tsukuba-shi 305, Japan

The kinetic analysis of the transformation of gels to α-alumina in the Al $(OPr^i)_3$–Al$(NO_3)_3$–(citric acid) system, was studied; the relationship between α-alumina and the gel structure, presumed from the solution structure and the transformation to α-alumina by calcination, was also investigated. It was shown that the gel structure effects the formation of α-alumina nuclei and their growth. The former was confirmed by the apparent activation energy obtained from incubation time, namely the gel obtained from the spinnable solution showed a smaller apparent activation energy than that from the unspinnable solution. Evidence for the latter was derived from the apparent activation energy, obtained from annealing time. That is, contrary to above, the gel obtained from the spinnable solution showed a larger apparent activation energy. However, the gel structure did not affect the manner of crystal growth. These phenomena can be explained by the difference in gel structure, i.e. by the kind of Al–O structure it is composed of, and by the conditions of formation of the α-alumina grains in the first place.

1. Introduction

In a previous investigation, alumina fibres were prepared by precursor methods from aqueous solutions of Al$(OPr^i)_3$–AlCl$_3$–citric acid (method A), Al$(OPr^i)_3$–AlCl$_3$ (method B), Al$(OPr^i)_3$–Al $(NO_3)_3$–citric acid (method C) and Al$(OPr^i)_3$–Al$(NO_3)_3$ (method D) [1], where correlation between solution structure and spinnability, to obtain gel fibres, was determined by nuclear magnetic resonance (NMR) of these solutions. In another paper, this correlation was studied by small-angle X-ray scattering (SAXS) [2]. Although amorphous gel structures usually formed from these solutions, it was not possible to analyse the structures in detail directly because line broadening made resolution of curves difficult even after magic angle spinning (MAS–NMR) measurement. However, it was expected that the gel microstructures reflected the solution structures resulting from the composition and the preparation procedure.

Accordingly, it is presumed that the transition condition for alumina to be formed from previously described gels would differ depending on calcination, and that the transformation kinetics to α-alumina would affect it. The decomposition of the Al structure and of organics in the gel during heat treatment have been reported previously [3], but no report is seen dealing with the influence of gel structure of gel structure on crystal transformation kinetics, as seen in mullite formation; although, there are reports available on the binary system [4–7].

In the present paper, the kinetic analysis of α-alumina gel transformation, obtained by methods C and D previously described, i.e. in the Al$(OPr^i)_3$–Al $(NO_3)_3$–(citric acid) system, was studied. The relationship between the gel structure, expected from solution structure, and the transformation to α-alumina by calcination was investigated. Kinetic analysis of gels obtained by methods A and B, i.e. in the Al$(OPr^i)_3$–AlCl$_3$–(citric acid) system, will be published in the near future.

2. Experimental procedure
2.1. Preparation of dry gel

Al$(OPr^i)_3$–Al$(NO_3)_3$–citric acid and Al(OPr^i)–Al$(NO_3)_3$ system dry gels were prepared for kinetic analysis by the following procedure. Aqueous solutions, which could be condensed to solution with or without spinnability and further consolidated to dry gel, were prepared in the manner reported previously [1]. The preparation procedure for dry gels is shown schematically in Fig. 1. The preparation systems for dry gels can be classified into two groups and four systems, as shown in Table I, according to spinnability, as classified before [1].

First, dry gel was obtained by spinnable solution in NCS and by unspinnable solution in NC. The Al$(NO_3)_3$·9H$_2$O obtained was dissolved in distilled water, so that the molar ratio of H$_2$O to total Al should be 50:50 in both systems. Then, Al$(OPr^i)_3$ was

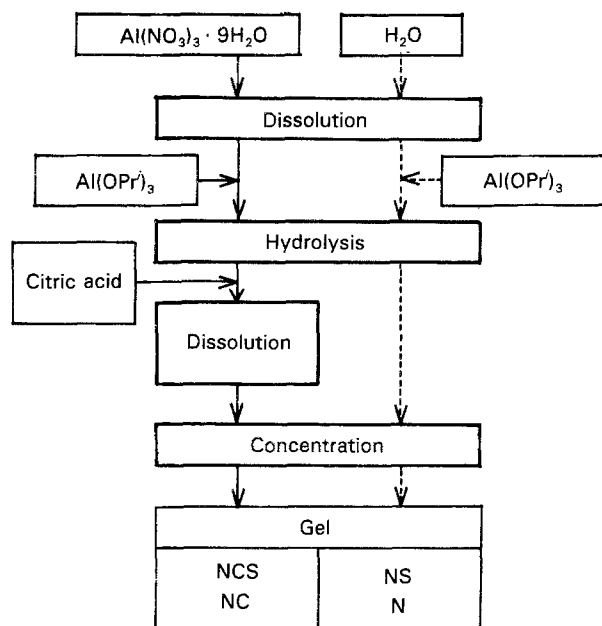*Figure 1* Fabrication processes of gel specimen.

TABLE I Outline of systems employed in this work

	Al(OPr^i)3(mol %) Al(NO$_3$)$_3$(mol %)	Citric acid	Spinnability
NCS	2	O	O
NC	5	O	X
NS	2	–	O
N	5	–	X

added slowly to this solution, stirring at room temperature so that the molar ratio of Al(OPr^i)$_3$ to Al(NO$_3$)$_3 \cdot$9H$_2$O should be 2 in the NCS system, and 5 in the NC system. These solutions were stirred at room temperature for one night, and citric acid monohydrate 1:10 mol to total Al mol was dissolved in both solutions. Then, these solutions were condensed to viscous sol, or jelly, in an oil bath at 100 °C. These mass were dried to gels in a 105 °C oven, then ground to fine powder for further experimentation.

In NS, from which dry gel was obtained by spinnable solution, and in N by unspinnable solution, the preparation procedure and the composition were the same as in the NCS and NC systems described above, respectively, without the addition of citric acid.

2.2. Quantitative X-ray diffraction analysis

The degree of transformation was determined by measuring the wt % of α-alumina by quantitative XRD analysis, using RAD-γ B (Rigaku Denki Co.) with graphite monochrometer CuK$_\alpha$ radiation at 50 kV 200 mA. The sample holder was an engraved glass plate, into which the sample powder was pressed with a glass slide, following essentially the procedure of Klug and Alexander [8]. The percentage conversion was determined from the integration intensity of the area under characteristic diffractogram peaks. Integrated intensity readings were taken at 2θ ranges from 24.0 to 26.5°, and the integrated baseline in-

tensities were also recorded for each scan and subtracted from their respective peaks.

This intensity was converted to the wt % of α-alumina by comparison with a previously determined calibration curve. The calibration curve was established by using prescribed mixtures of α-alumina and γ-alumina ranging between 10–90 wt %. γ-alumina was used for calibration because it would definitely be present in the in calcination of gels prepared in this paper. According to our analysis, estimation can be achieved within ± 2 wt % accuracy.

2.3. Dry gel isothermal treatment

First, 2.0 g of dry gel powder was put into a Pt crucible, which was then loaded into a hot furnace preheated to 600 ± 1 °C. The powder was withdrawn from the furnace 10 min later. This preheat treatment was performed in order to remove volatile components, such as H$_2$O and organics, beforehand. Then, the crucible was loaded in a hot furnace heated at 950–1050 ± 1 °C, restabilizing the furnace temperature a few minutes later. The crucible was withdrawn from the hot furnace to anneal from 1 to 24 h. The isothermal transformation of gels maintained at 700, 800, 1000 and 1100 °C for 1 h were observed by X-ray diffraction (XRD).

The microstructure of specimens obtained with different α-alumina conversions were observed by scanning electron microscopy (SEM).

3. Results and discussion

3.1. Phase transformation by isothermal annealing

Fig. 2 shows XRD patterns of NCS gels which were treated isothermally at 700, 800, 1000 and 1100 °C for 1 h. The XRD pattern of gels treated at 700 °C
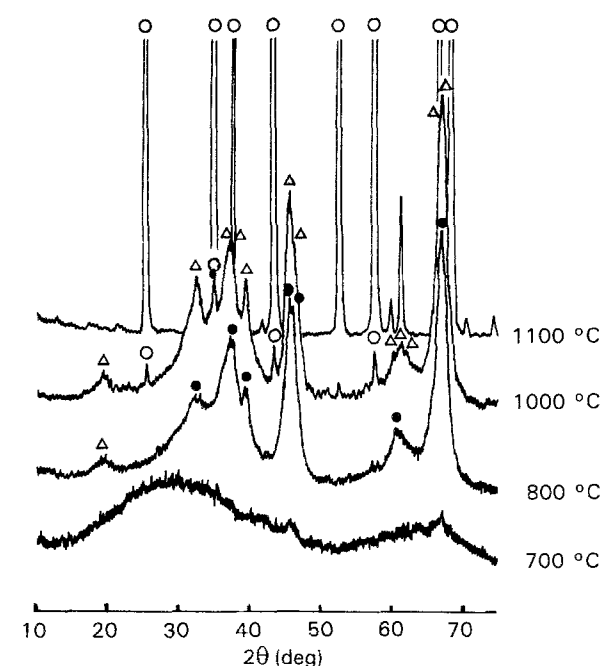

Figure 2 X-ray diffraction patterns of NCS specimen calcined at respective temperatures for 1 h. (●) γ-Al$_2$O$_3$, (△) θ-Al$_2$O$_3$, (O) α-Al$_2$O$_3$.

shows an amorphous phase and indicates the transformation of γ-alumina to α-alumina through to θ-alumina at higher temperature. Similar transformations were detected for NC, NS and N specimens.

3.2. α-alumina formation kinetics

In Figs 3–6, weight fractions of α-alumina in isothermally annealed NCS, NC, NS and N specimens, determined quantitatively by X-ray diffraction analysis, are shown versus annealing time for various temperatures. For each specimen, it was indicated that the higher the temperature of isothermal treatment, the shorter the time required for complete transformation to α-alumina. Also, the weight per cent conversion to α-alumina increases sigmoidally with annealing time. Accordingly, a nucleation and growth kinetic model can be applied to each specimen. The transformation data can be described by an Avrami–Erofeev kinetic equation [9]

$$\alpha = 1 - \exp\left(-K \cdot t_{ann}^n\right) \qquad (1)$$

Transformed into linear form Equation 1

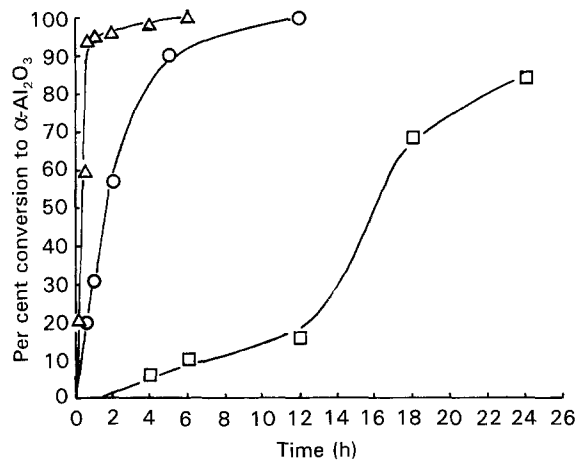$$\ln\ln\left(1/1 - \alpha\right) = \ln K + n\ln t_{ann} \qquad (2)$$

Figure 3 Isothermal α-alumina transformation curves at various temperatures for NCS specimen. ($\triangle$), ($\bigcirc$), ($\square$).
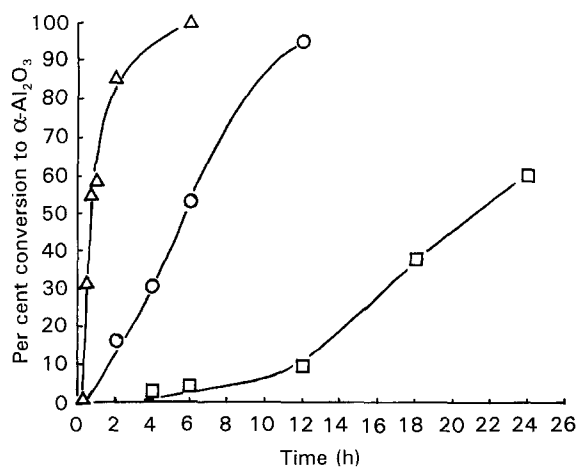

Figure 4 Isothermal α-alumina transformation curves at various temperatures for NC specimen. ($\triangle$), ($\bigcirc$), $\square$.
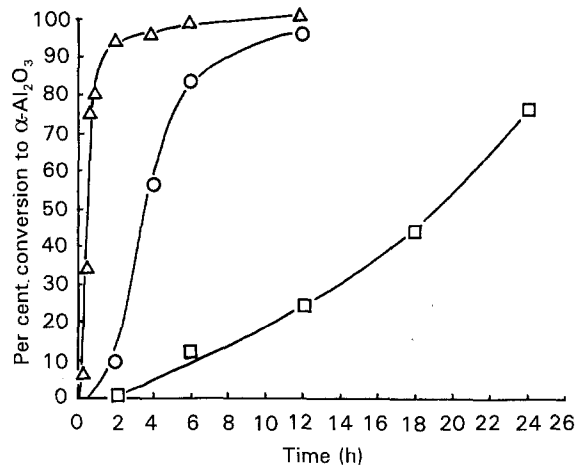
Figure 5 Isothermal α-alumina transformation curves at various temperatures for NS specimen. ($\triangle$), ($\bigcirc$), ($\square$).
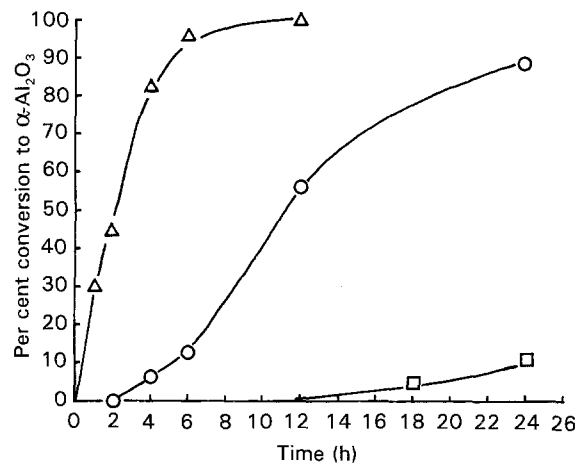
Figure 6 Isothermal α-alumina transformation curves at various temperatures for N specimen. ($\triangle$), ($\bigcirc$), ($\square$).

Here α is the per cent conversion to α-alumina; t_{ann} the actual annealing time; K the rate constant, which depends upon the nucleation and growth rates, and n is a so-called time exponent or time constant, which relates to the manner of crystal growth.

However, it was shown that the transformation is preceded by an incubation time for all temperatures and specimens. The incubation time, τ_{inc}, was estimated by extrapolating the line given by plotting $\ln\ln$ $(1/1 - \alpha)$ against $\ln t_{ann}$ to the 2 wt % transformation level, because of ± 2 wt % accuracy, and noting the corresponding time. The obtained incubation times are listed in Table II. Here for NCS, NC, NS and N specimens, if an Arrhenius type plot of $\ln \tau_{inc}^{-1}$ against $1/T$, where T represents an absolute annealing temperature, gives a straight line, the incubation can be consolidated to involve an activated process with an apparent activation energy of α-alumina nuclei formation. As shown in Fig. 7, NCS, NC, NS and N specimens give straight lines, with correlation coefficients of more than 0.99 by least squares, to result in apparent activation energies of 420, 430, 405 and 526 KJ mol^{-1}, respectively. Except for the N specimen these values are in certain agreement with the energy, 395 KJ mol^{-1}, for α-alumina to appear from boehmite

TABLE II Incubation times estimated by the extrapolation of ln ln $(1/1 - \alpha)$ versus ln t_{ann} plot to 2 wt % α-alumina for various annealing times

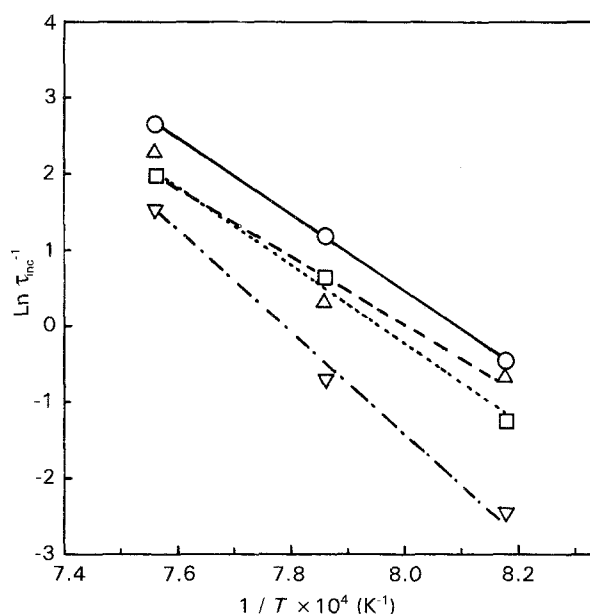|	Temperature (°C)	Incubation time (hr)
	950	1.64
NCS	1000	0.31
	1050	0.07
	950	3.47
NC	1000	0.54
	1050	0.14
	950	2.03
NS	1000	0.73
	1050	0.10
	950	11.77
N	1000	2.16
	1050	0.23

Figure 7 Arrhenius plot of incubation time versus annealing temperature for (O) NCS, (□) NC, (△) NS and (▽) N specimens.

[10]. Also, it is noticed from these values that: first, specimens obtained from unspinnable solutions (NC, N) give higher apparent activation energies than spinnable ones (NCS, NS): second, specimens obtained from spinnable solutions (NCS): second, specimens obtained from spinnable solutions (NCS), to which citric acid is added, give higher apparent activation energies than those to which acid has not been added (NS). The former suggests that differences in gel structure, deduced from solution structure, affects α-alumina nucleation. Namely, gel specimens such as NC and N have a more inhomogeneous Al–O structure than NCS and NS, respectively, as already reported [1, 2].

The inhomogenity of the Al–O structure is believed to be due to clusters such as the Al_{13}^{7+} polycation, which is composed of tetragonal and octagonal Al–O bonds, that are considered to fix in gel. This inhomogenity affects the transformation accompanying the coordination change to γ-alumina, or further to a

metastable phase, for example θ-alumina; then finally inhibits the nucleation of α-alumina. In this way, it is considered that the gel structure affects the transformation kinetics up to the last stable phase. The latter suggests that the presence of residual carbon, resulting from citric acid, prohibits the nucleation of α-alumina similarly to the case of mullite [5].

Some the weight per cent conversion to α-alumina increases sigmoidally with annealing time, t_m, where $t_m = t_{ann} - \tau_{inc}$, Equation 2 is transformed into Equation 3

$$\ln\ln (1/1 - \alpha) = \ln K + n\ln t_m \qquad (3)$$

The plot of ln ln $(1/1 - \alpha)$ against ln t_m for the NCS specimen is shown in Fig. 8. This plot gives a straight line, which indicates a time exponent value of 1.6. All the other specimens, such as NC, NS and N, also show the same time exponent value of 1.6, although they are not shown here. It is made clear that the gel structure does not affect the manner of crystal growth.

Fig. 9 shows an Arrhenius type plot of ln K against $1/T$ for NCS, NC, NS and N specimens, where K is a rate constant obtained from Equation 3. Each NCS, NC, NS and N specimen gives a straight line with a correlation coefficient of more than 0.99, by least squares, to result in apparent activation energies of 473, 408, 452 and 415 KJ mol^{-1}, respectively. These apparent activation energies essentially contain the activation energy of growth of α-alumina grains and the nucleation of α-alumina. But, there are reports on the independence of a number of α-alumina nuclei from the annealing time [11–13]. Accordingly, these apparent activation energies indicate the activation energy of growth of α-alumina grains. Comparing apparent activation energies obtained here with those obtained from the incubation time, the transformation from gel to α-alumina is growth controlled for NCS and NS specimens, while it is nucleation controlled for NC and N specimens. It is reported that the α-alumina transformation kinetics from boehmite, which possesses octahedral Al–O structure, is growth controlled,
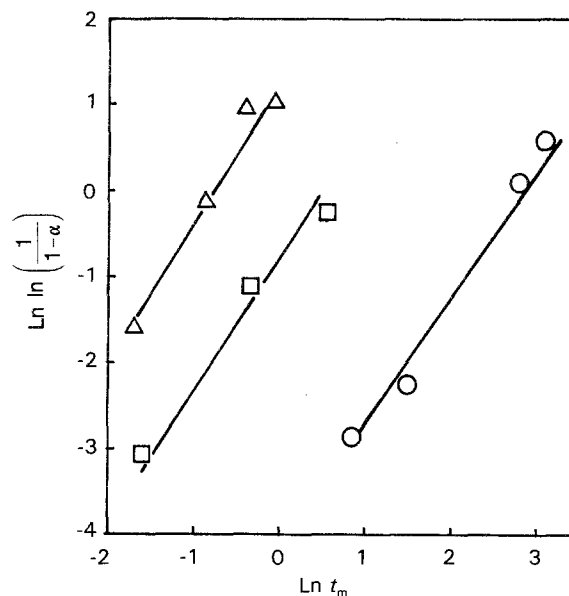

Figure 8 Conversion results for NCS specimen plotted according to the Avrami model for (O) 950 °C, (□) 1000 °C, (△) 1050 °C.
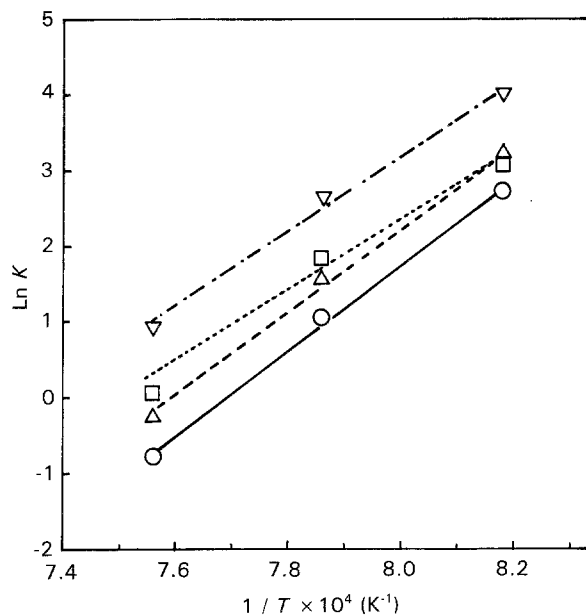
Figure 9 Arrhenius plot of annealing time minus incubation time versus annealing temperature for (○) NCS, (□) NC, (△) NS and (▽) N specimens.

and that it gives an apparent activation energy of 431 KJ mol^{-1} [11]. Accordingly, it is considered that NCS and NS specimens, which are considered to possess a relatively homogeneous Al–O structure, transform to α-alumina in growth controlled manner, the same as for boehmite. To the contrary, the transformation of NC and N specimens, which are considered to possess a relatively inhomogeneous Al–O structure, to α-alumina are governed by the formation of nuclei described above. This can be supported by the observation of microstructures mentioned below.

Fig. 10 shows SEM images of NCS and NC specimen microstructures before and after annealing at 950 °C for various times. It can be seen that in the NCS specimen annealed for 6 h (Fig. 10b), of which

per cent conversion to α-alumina is 11, α-alumina forms spherical colonies in which grains, having diameters between 0.05–0.1 μm, and innumerable pores are seen. After sintering for 18 h (Fig. 10c), the per cent conversion to α-alumina rises to 68. It can be seen that there are grains having diameters of 0.2 μm in a fraction of the colonies, and that grains grew to a certain extent with the vermicular microstructure; but grains having diameters between 0.05–0.1 μm can still be seen.

On the other hand, in the NC specimen annealed for 12 h (Fig. 10e), of which per cent conversion to α-alumina is 10, the grains are ∼ 0.05 μm in diameter and have a slightly vermicular structure. After annealing for 24 h (Fig. 10f), the per cent conversion to α-alumina is 59, α-alumina grains between 0.1–0.25 μm in diameter form colonies with vermicular structure. It is considered that these surroundings grow α-alumina having diameters larger than 0.3–0.4 μm judging from the porous structure.

As shown above, it is indicated that initial α-alumina nuclei formation in the NCS specimen gives higher porosity than in the NC specimen, i.e. the NCS specimen has a lower nucleating density than the NC specimen. Because the NCS specimen, compared to the NC specimen, has a porous structure composed of mostly isolated and small α-alumina grains following initial annealing, the growth of each α-alumina crystal was severely hampered by reduced contact between particles in the porous structure and by enhanced diffusion resistance at the phase boundary in small grains. Accordingly, it is considered that the NCS specimen has a higher apparent activation energy, obtained from ln K against 1/T plots, than the NC specimen. These relationships also hold for the NS and N specimens.

As described above, it was shown that the Al–O structure in the gel affects the initial formation of α-alumina nuclei and their densities. The situation is
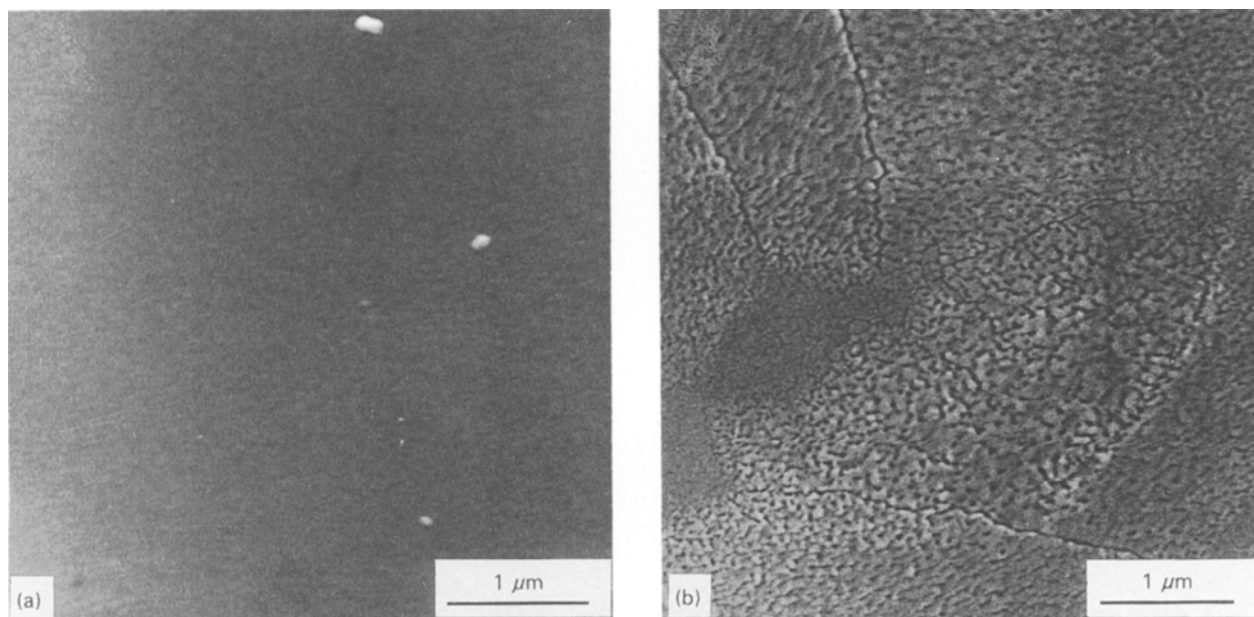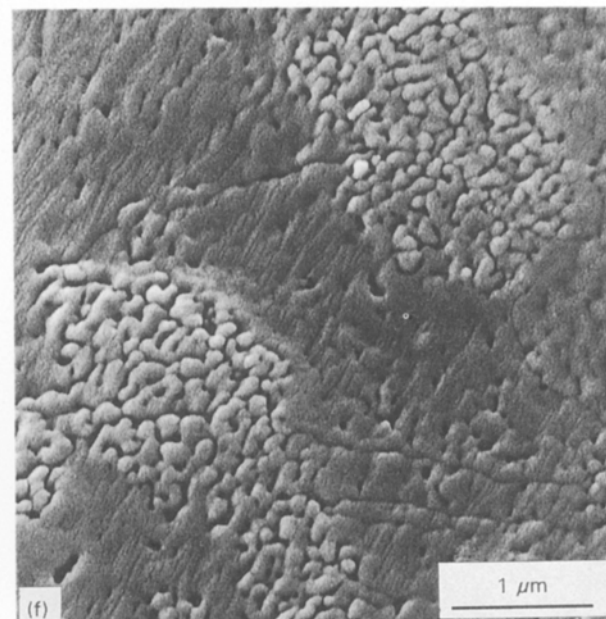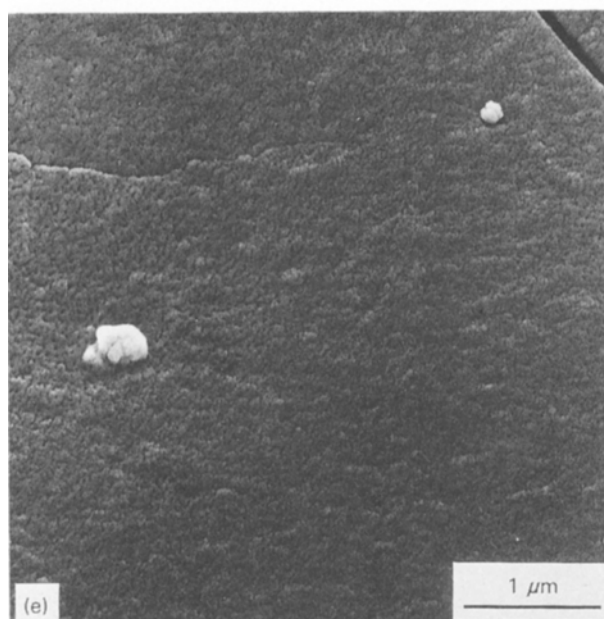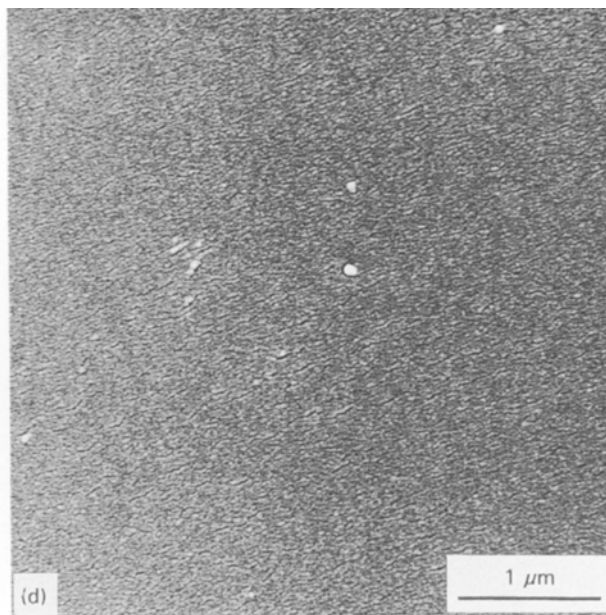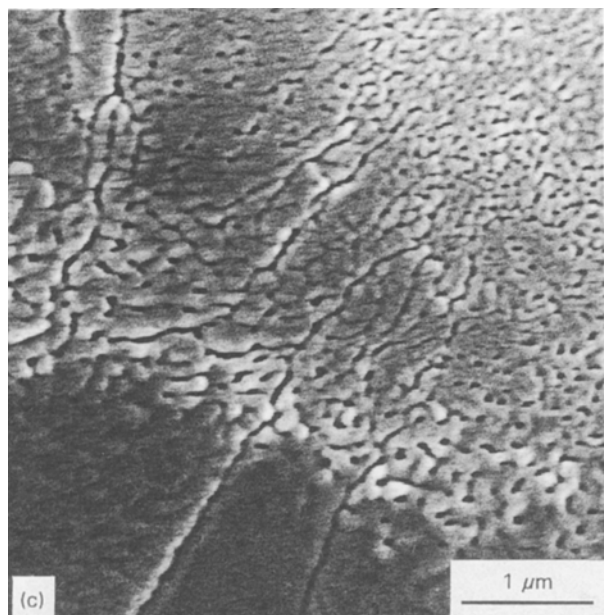

Figure 10 Microstructure of NCS and NC specimens annealed at 950 °C for various times. NCS specimen: (a) preheated (600 °C 10 min) gel before annealing, (b) annealed for 6 h (11 wt % conversion to α-alumina), (c) annealed for 18 h (68 wt %). NC specimen: (d) preheated (600 °C 10 min) gel before annealing, (e) annealed for 12 h (10 wt %), (f) annealed for 24 h (59 wt %).

(c)   1 μm

(d)   1 μm

(e)   1 μm

(f)   1 μm

such that the initial formation density of α-alumina nuclei affect grain growth. Accordingly, because NCS and NS specimens (which show lower apparent activation energies, obtained from the slope of $\ln \tau_{inc}^{-1}$ against $1/T$, than NC and N specimens) generate many isolated α-alumina nuclei, the apparent activation energy obtained from the slope of $\ln K$ against $1/T$ is higher than for NC and N specimens.

In this way, it was shown that the difference in gel structure does not affect the manner of crystal growth, but affects the formation of the final stable phase through the intermediate and metastable phase by annealing.

4. Conclusions

The kinetic analysis of gels for α-alumina transformation in the $Al(OPr^i)_3$–$Al(NO_3)_3$–(citric acid) sys-

tem was studied to clarify the relationship between gel structure expected by solution structure, and the transformation to α-alumina for calcination. The following results were obtained:

1. Transformation is preceded by incubation; which is an activated process, with apparent activation energies of 420, 430, 405 and 526 $KJ\,mol^{-1}$ for NCS, NC, NS and N specimens, respectively.

2. An Avrami equation can be applied to the transformation kinetics, analysed quantitatively by X-ray diffraction with a time exponent of 1.6, in all specimens by subtracting the annealing time from the incubation time. It was concluded that the gel structure does not affect the manner of crystal growth.

3. The apparent activation energy obtained from the slope of $\ln K$ against $1/T$ is 473, 408, 452 and 415 $KJ\,mol^{-1}$ for NCS, NC, NS and N specimens, respectively.

4. α-alumina is formed via nucleation control for NC and N specimens, and by growth control for NCS and NS specimens. The gel structure affects the initial formation and growth of α-alumina nuclei.

References

1. T. NISHIO and Y. FUJIKI, *J. Chem. Soc. Jpn* **99** (1991) 1346.
2. *Idem., ibid.* to be published.
3. M. S. LIZER and S. PAWLOWSKI, "High Tech Ceramics" (Elsevier Science, 1987) p. 2327.
4. J. C. HULING and G. MESSING, *J. Amer. Ceram. Soc.* **74** (1991) 2374.
5. D. X. LI and W. J. THOMSON, *ibid.* **73** (1990) 964.
6. *Idem., J. Mater. Res.* **5** (1990) 1963.
7. W. C. WEI and J. W. HALLORAN, *J. Amer. Ceram. Soc.* **71** (1988) 581.
8. H. P. KLUGG and L. K. ALEXANDER in "X-ray diffraction procedures" 2nd Edn (John Wiley, New York, 19) p. 531.
9. M. YOSHIMURA, M. HAYAKAWA and S. SOMIYA, *J. Ceram. Soc. Jpn.* **97** (1989) 1339.
10. S. J. WILSON and J. D. C. MCCONNEL, *J. Solid. St. Chem.* **34** (1980) 315.
11. R. A. SHELLEMAN, G. L. MESSING and M. KUMAGAI, *J. Non-Cryst. Solids* **82** (1986) 277.
12. F. W. DYNYS and J. W. HALLORAN, *J. Amer. Ceram. Soc.* **65** (1982) 442.
13. K. HAYASHI, S. TOYODA, H. TAKEBE and K. MORINAGA, *J. Ceram. Soc. Jpn.* **99** (1991) 550.